INTEGRAL/IBIS Results on Gamma-Ray Polarization

D. Götz, P. Laurent, J. Rodriguez, P. Moran, …

CEA Salcay DSM/Irfu/SAp-AIM

Plan

- INTEGRAL
- Polarimetry with IBIS
- Gamma-Ray Bursts (041219A, 061122, 120711A, 140206A)
  - Polarization & LIV
- Compact Objects
  - Crab
  - Cyg X-1

The INTErnational Gamma-Ray Astrophysics Laboratory

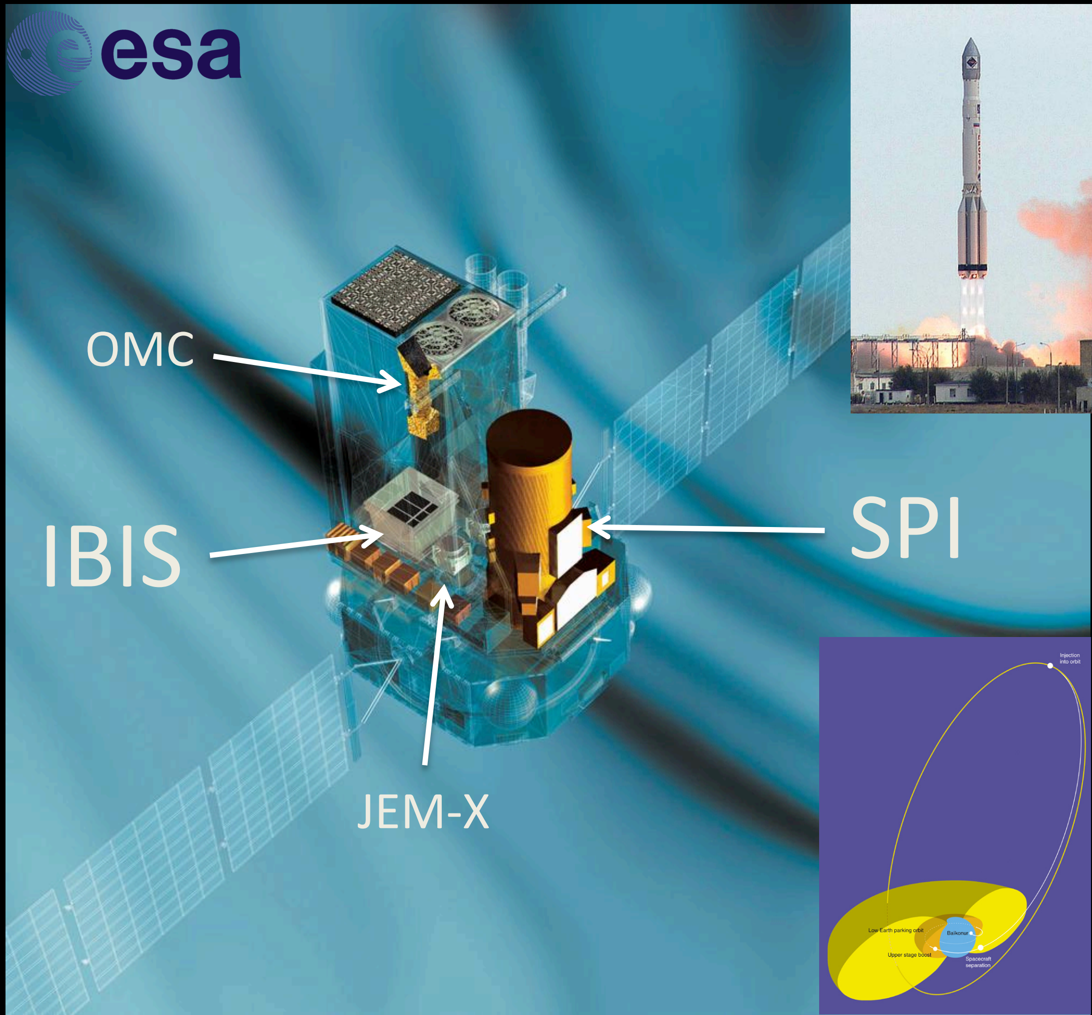

Launched on October 17th 2002 in an inclined (51.6°) ~3 days orbit (apogee: 9000 km, perigee 153000 km). ESA mission with contributions from NASA and RKA.

Carries two main instruments, based on coded mask imaging technique: the “imager” IBIS (15 keV-10 MeV, 12 arc min PSF) and the “spectrometer” SPI (20 keV-8 MeV, ΔE=2.2 keV (FWHM) @ 1.33 MeV).

X-ray (JEM-X) and an optical (OMC) monitors are also present on board.

Polarimetry with IBIS

The IBIS Telescope

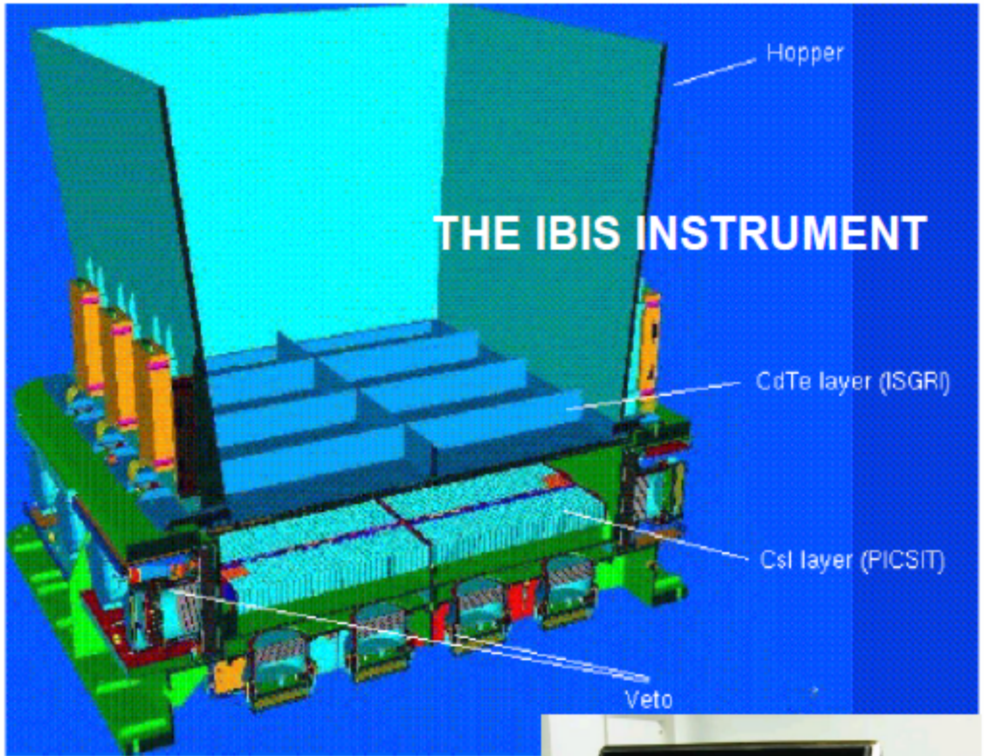

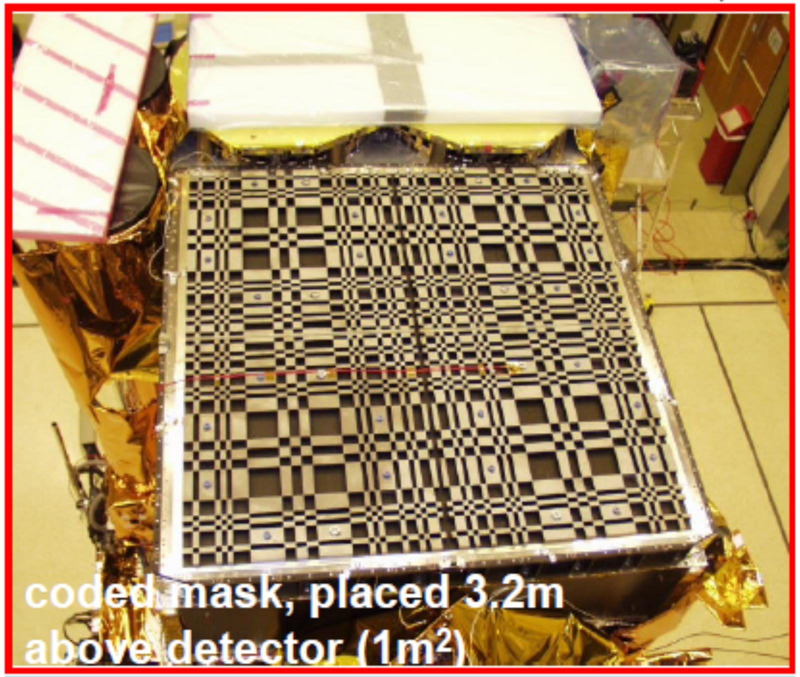

IBIS detector assembly:

two stacked detection planes, lateral and bottom veto anticoincidence, passive tungsten shield

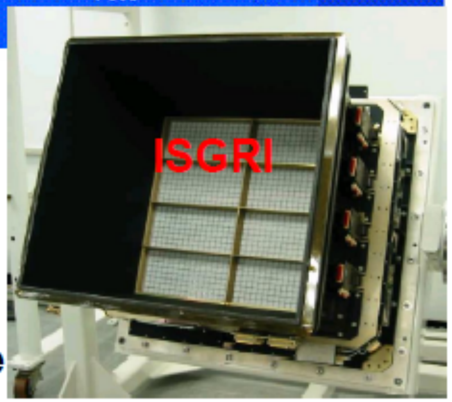

Collection area ~ 3000 cm^2

Two-Layers detector:

1) 2mm thick CdTe (ISGRI)

2) 30mm thick CsI (PICsIT)

Field-of-view: ±14.5° FWZR (± 4.5° fully coded)

IBIS as a Compton telescope

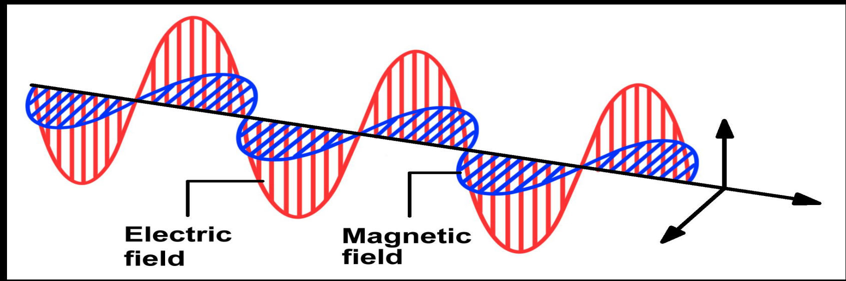

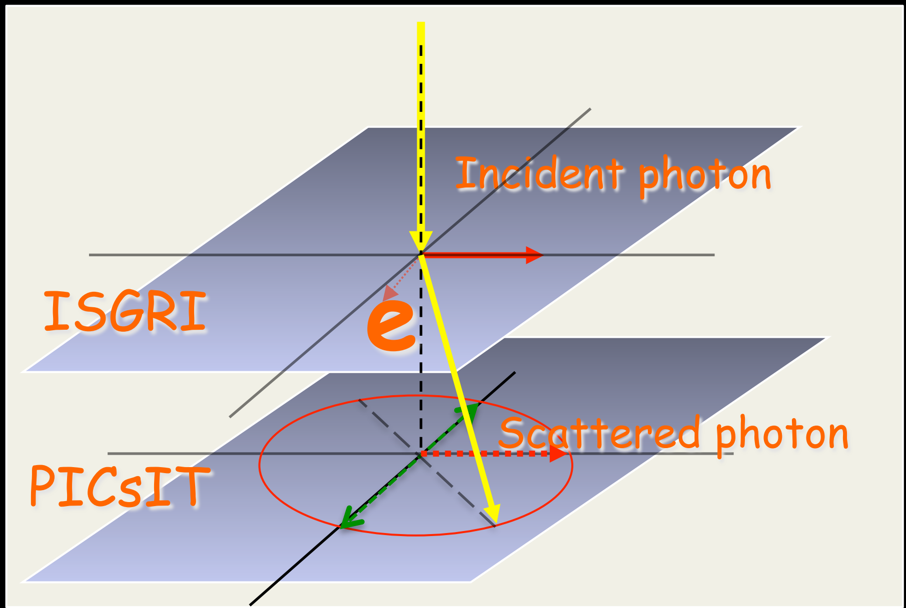

- The IBIS telescope is a coded mask telescope which could be used as a Compton telescope.
- The Compton mode events are ISGRI and PICSIT events in temporal coincidence, within a window $\tau_W \approx 3.8$ µs.

- Within this window, chance coincidence, called hereafter "spurious events", may also occur.

The IBIS Compton Telescope Advantages

It is a coded mask Compton telescope, so it takes advantage of the two imaging techniques:

- It produces sky images using the coded mask with the same capabilities as ISGRI.
- It has an inherent very low background (~ 90 cts/s) compared to SPI and PICsIT.
- We can use the Compton effect to further reduce the background, by selecting with the Compton kinetics, events coming only from the coded mask FOV.
- We can do polarimetry !

Compton Polarimetry Principles

• Compton scattering cross section is maximum for photons scattered at right angle to the direction of the incident electric vector ⇒ asymmetry in the azimuthal profile S of scattered events.

$$\frac{d\sigma}{d\Omega} = \frac{r_0^2}{2}\left(\frac{E'}{E_0}\right)^2\left(\frac{E'}{E_0} + \frac{E_0}{E'} - 2\sin^2\theta\cos^2\phi\right)$$

• Modulation:
  a = modulation factor
  polar. Fraction (PF) = a/a_{100}
  a_{100} = modulation for a 100 % polarized source.
  polar. angle = PA = $\varphi_0 - \pi/2 + n\pi$

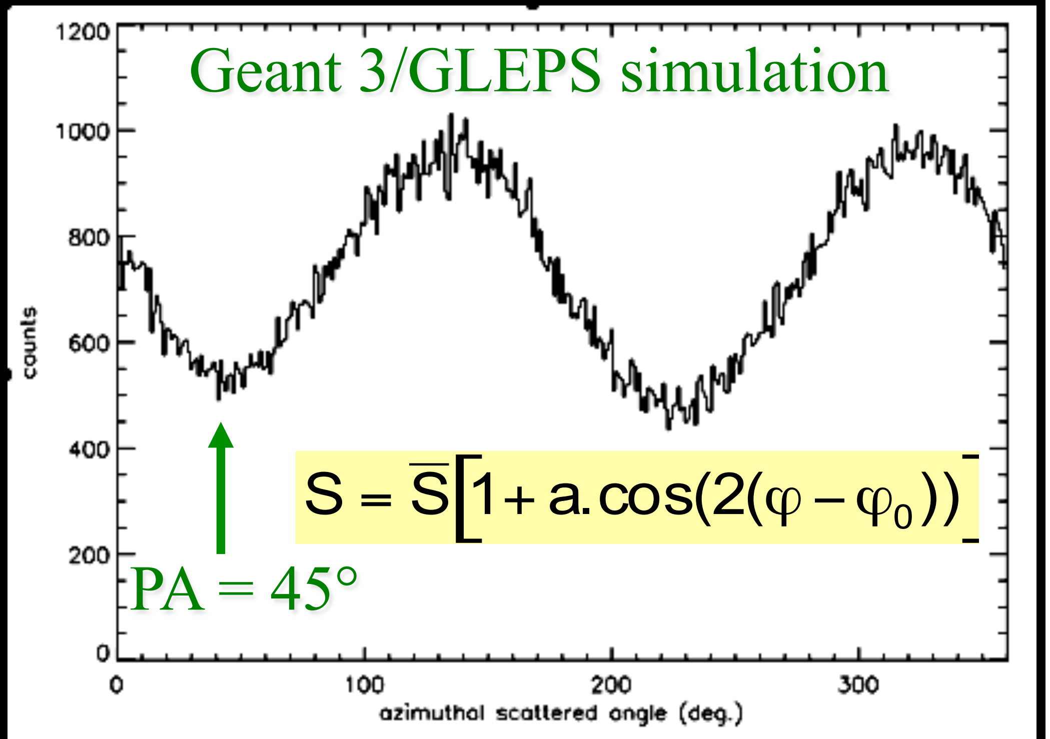

Image deconvolution

200-800 keV T=300 ks

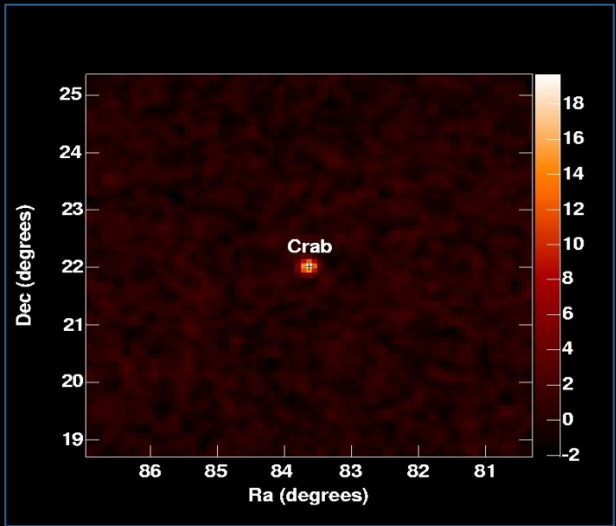

Shadowgram deconvolution

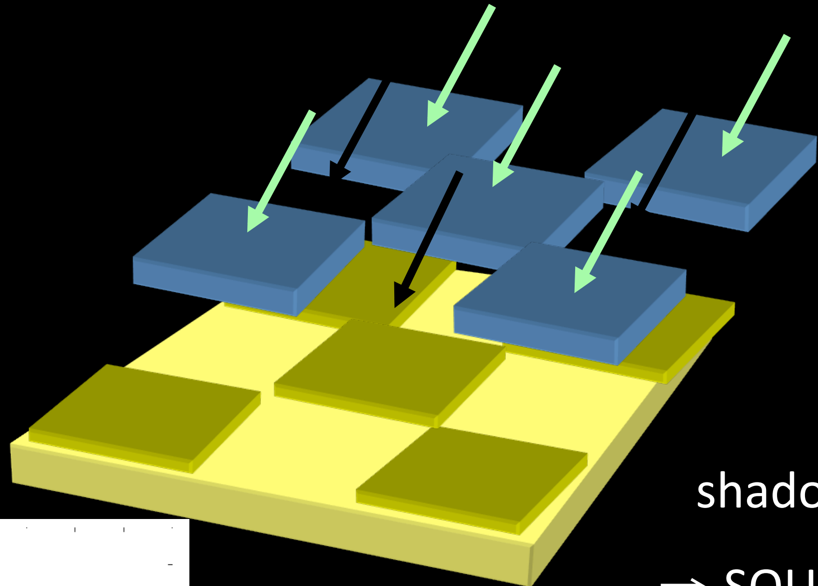

shadow

⇒ SOURCE DIRECTION

6 images by selecting the azimuthal scattering angle of the photons

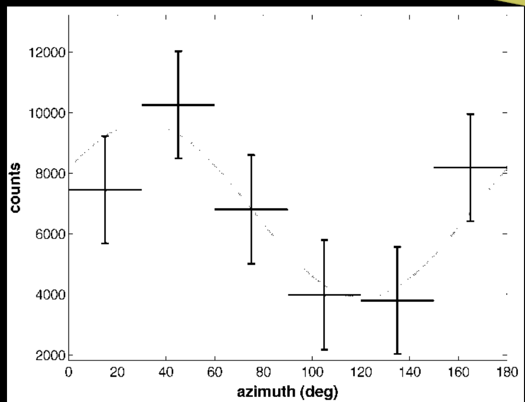

Gamma-Ray Bursts

GRB 041219

- Detected by the *INTEGRAL* Burst Alert System by triggering on its precursor
- Turned out to be a very long burst: T_{90}~460 s
- Very bright: fluence $_{20\text{-}200\ \mathrm{keV}}$ = 2.5 x10^{-4} erg cm^{-2} (top 1% of the BATSE sample)
- Two precursors and two main peaks
- Simultaneous NIR and optical flashes
- Measure of variable γ-polarization (Götz+09, McGlynn+07)

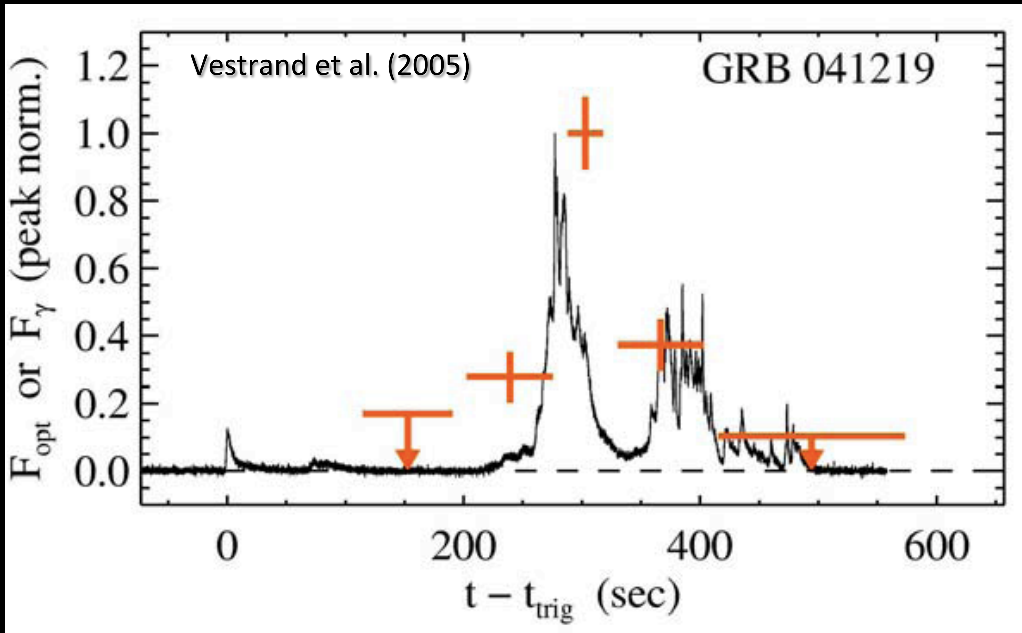

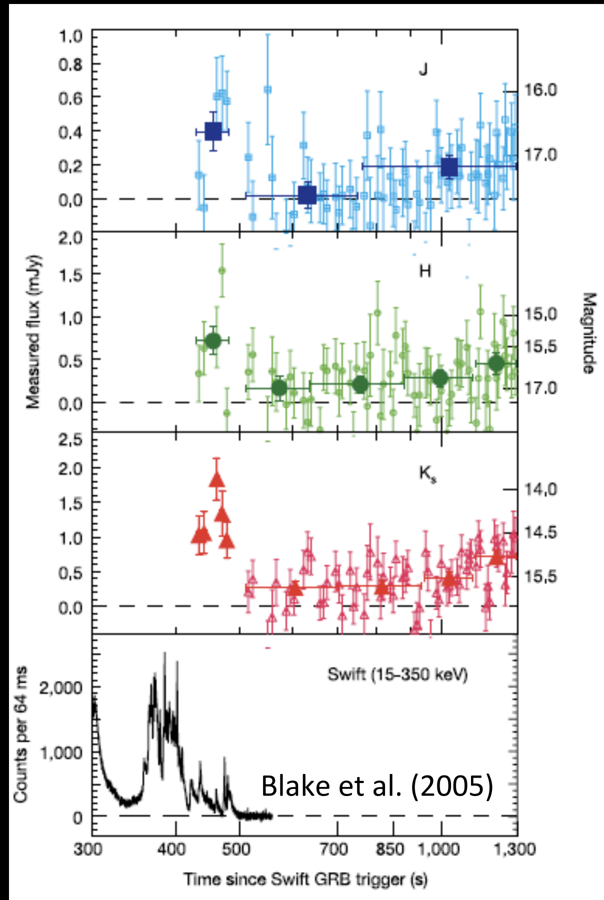

GRB 041219A: Compton mode light curve

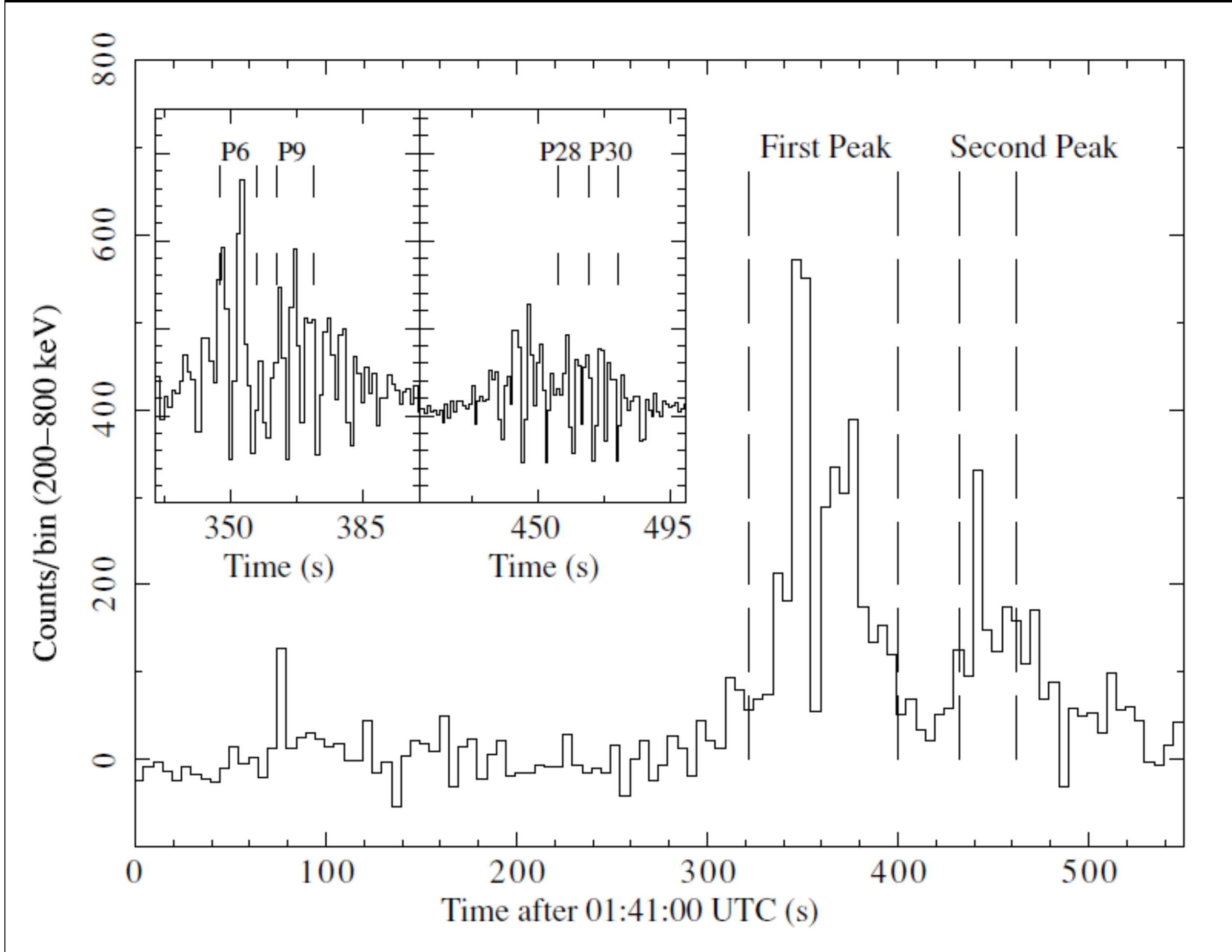

5s bins

Analysis in 10s bins

Total S/N (200-800 keV) 37 σ

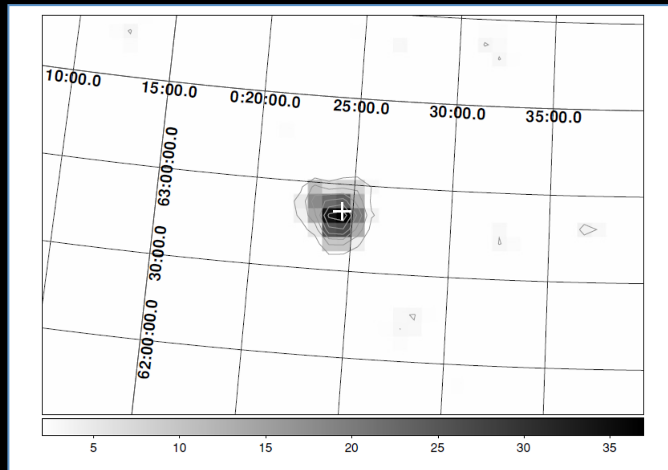

GRB 041219A: polarization results

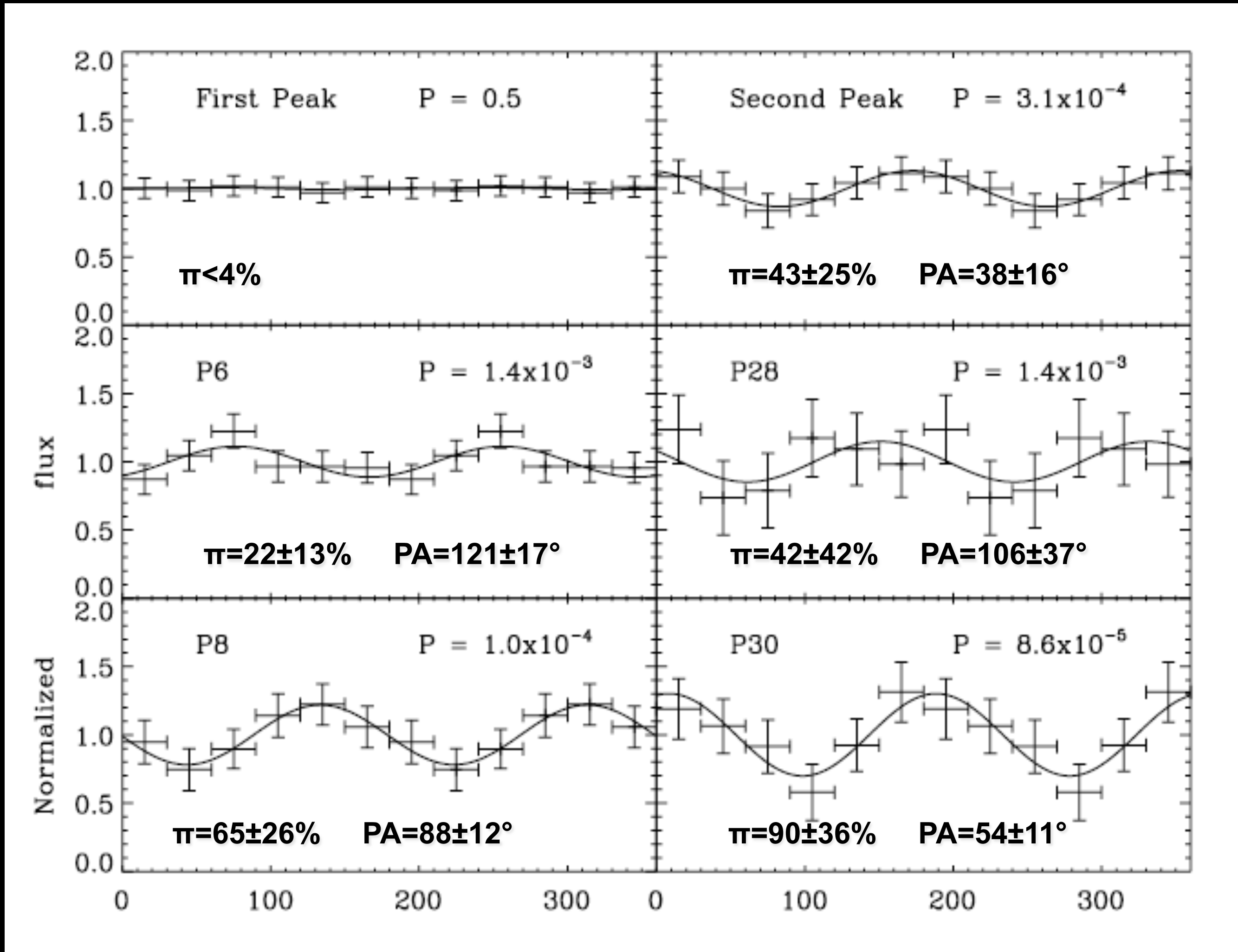

Götz+09

SPI: π=68±29% PA=70°$^{+19°}_{-27°}$

McGlynn et al. (2007)

041219A: polarization statistics

confidence levels at 67, 90, 95, and 99 %

Ao

Ao

Ao

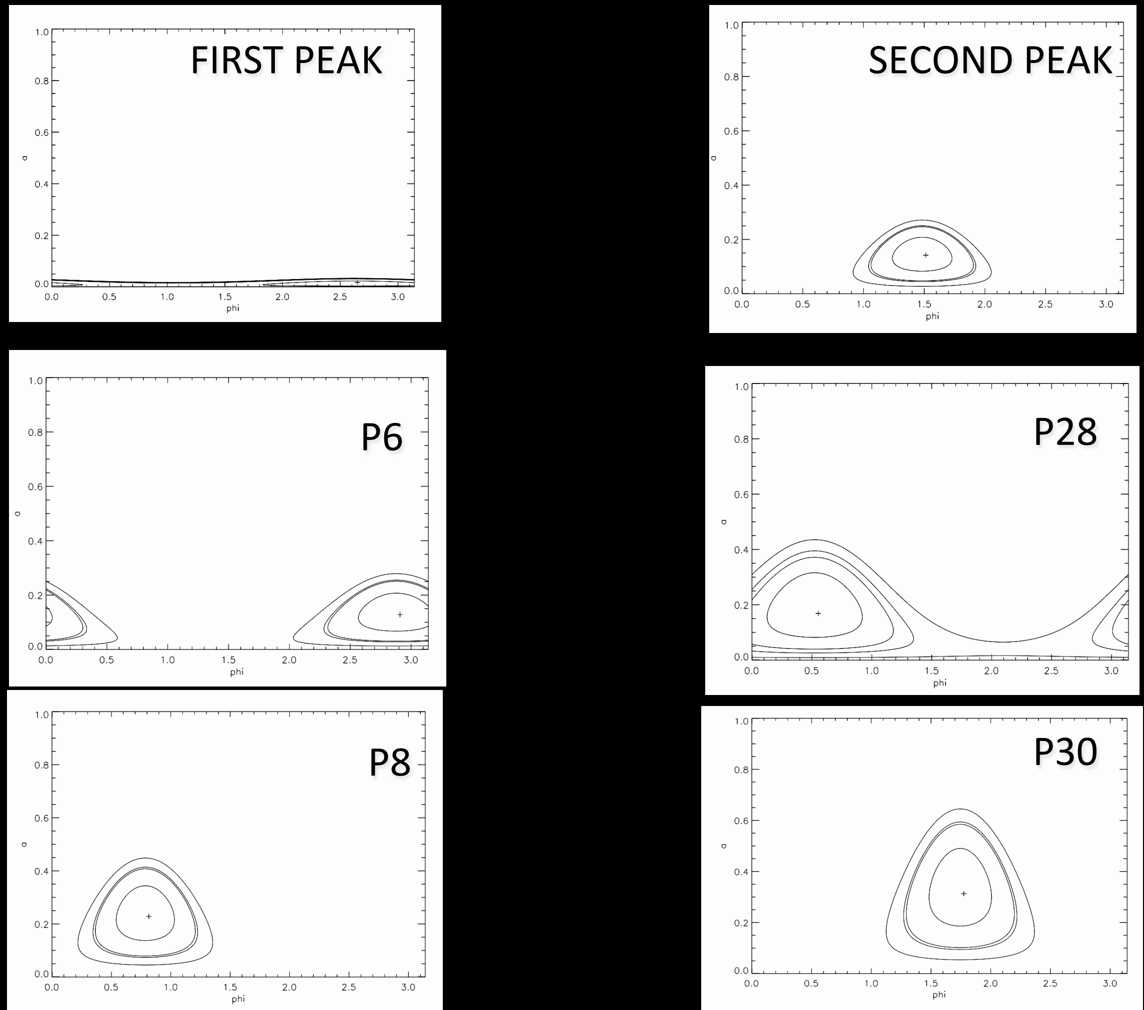

PHI0 PHI0

Interpretation(s)

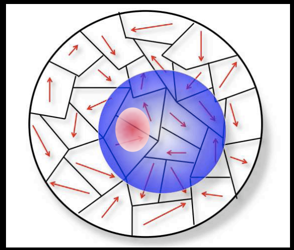

(i) synchrotron emission from shock accelerated electrons in a relativistic jet with magnetic field transverse to the jet expansion (Granot 2003, Granot & Königl 2003, Nakar, Piran & Waxman 2003)

(ii) synchrotron emission from purely electromagnetic flow (Lyutikov et al. 2003, Nakar, Piran & Waxman 2003)

(iii) synchrotron emission from shock accelerated electrons in a relativistic jet with a random magnetic field (Ghisellini & Lazzati 1999, Waxman 2003)

SAME POLARIZATION LEVELS AS IN (I) BUT A PECULIAR OBSERVATION CONDITION IS NEEDED
($\Theta_{obs} \cong \Theta_{jet}+k/\Gamma$)

(iv) Inverse Compton scattering from relativistic electrons in a jet propagating in a photon field ("Compton drag") (Lazzati 2004)

POLARIZATION LEVELS can reach 60-100% BUT ONLY UNDER THE CONDITION OF A NARROW JET ($\Gamma\Theta_{jet}$<5) AND THE SAME OBSERVATION CONDITIONS AS IN (iii) APPLY

(v) Independently from the emission process (synchrotron or inverse Compton), fragmented fireballs (shotguns, cannonballs, sub-jets) can produce highly polarized emission, with a variable P.A. The fragments are responsible for the single pulses and have different Lorentz factors, opening angles and magnetic domains. (e.g. Lazzati & Begelman 2009)

GRB 061122

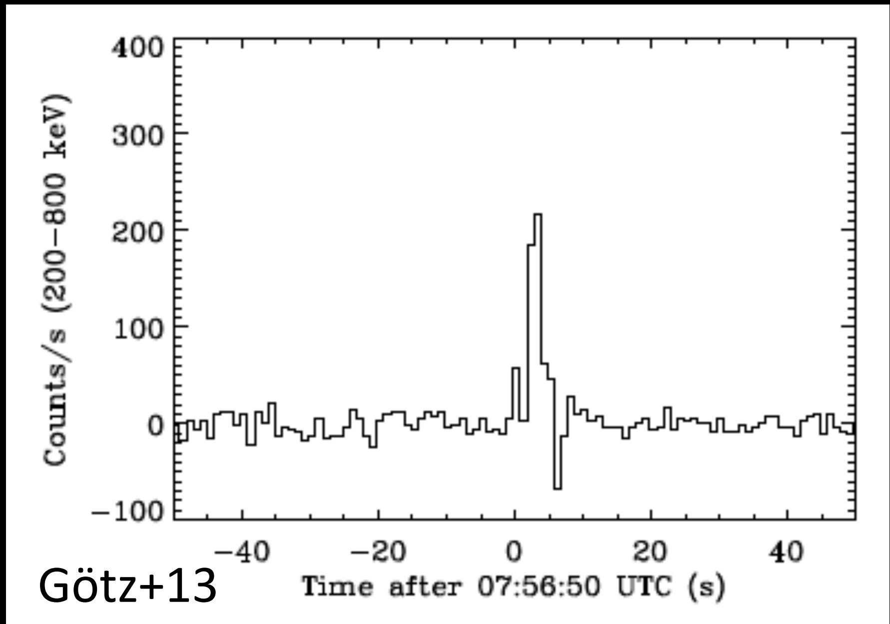

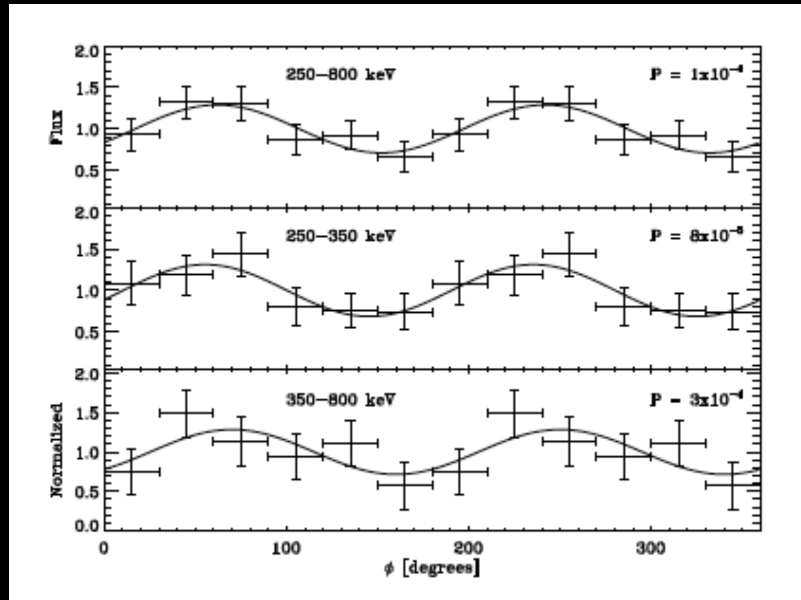

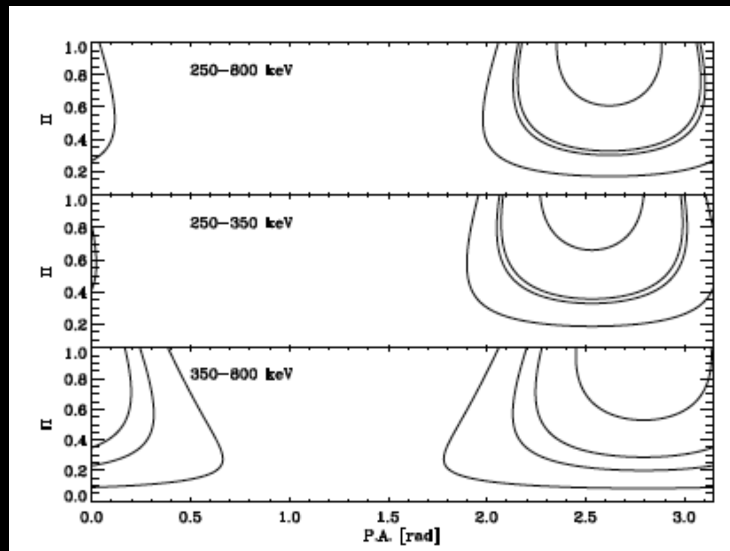

SPI u.l. < 60%McGlynn+09

Energy band (keV)	Π (%) (68% c.l.)	P.A. (°) (68% c.l.)	Π (%) (90% c.l.)	P.A. (°) (90% c.l.)
250–800	>60	150±15	>33	150±20
250–350	>65	145±15	>35	145±27
350–800	>52	160±20	>20	160±38

GRB 140206A

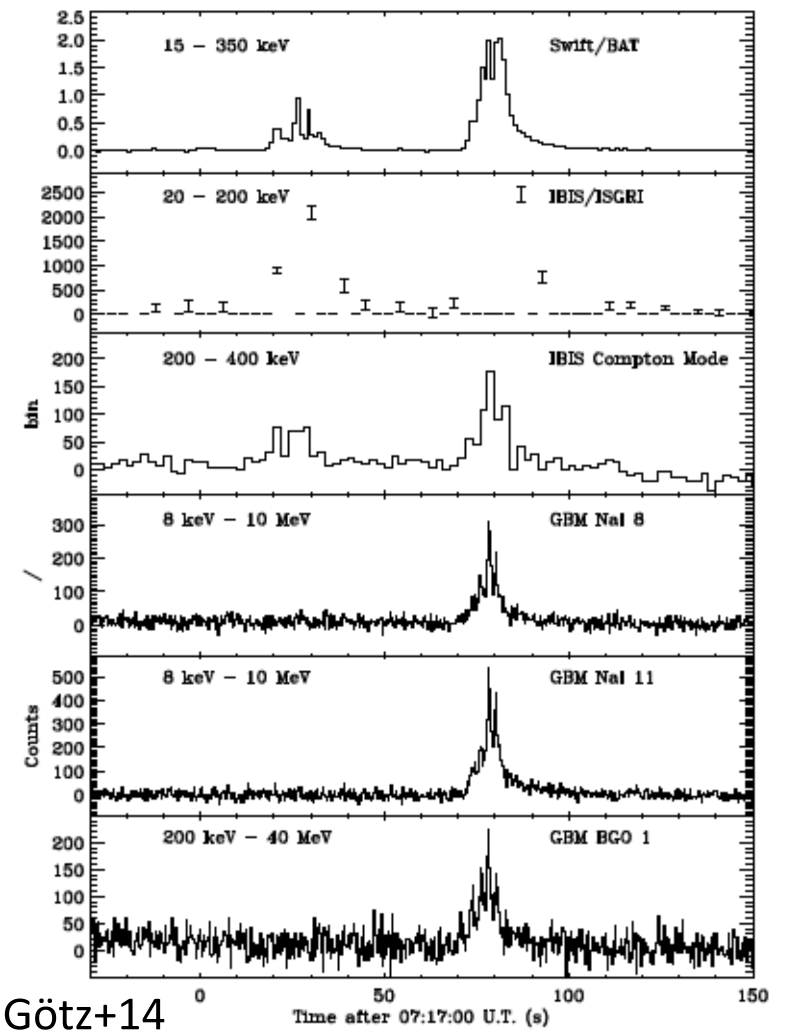

Götz+14

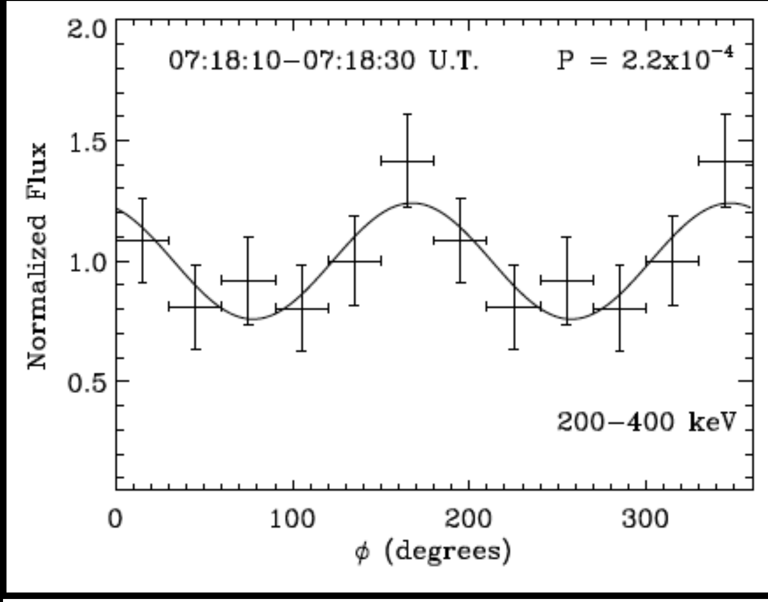

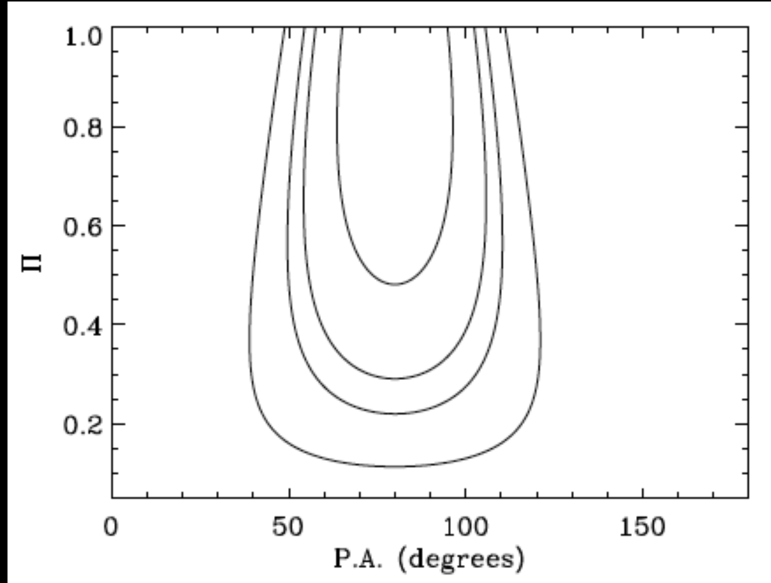

GRB 120711A (to be submitted)

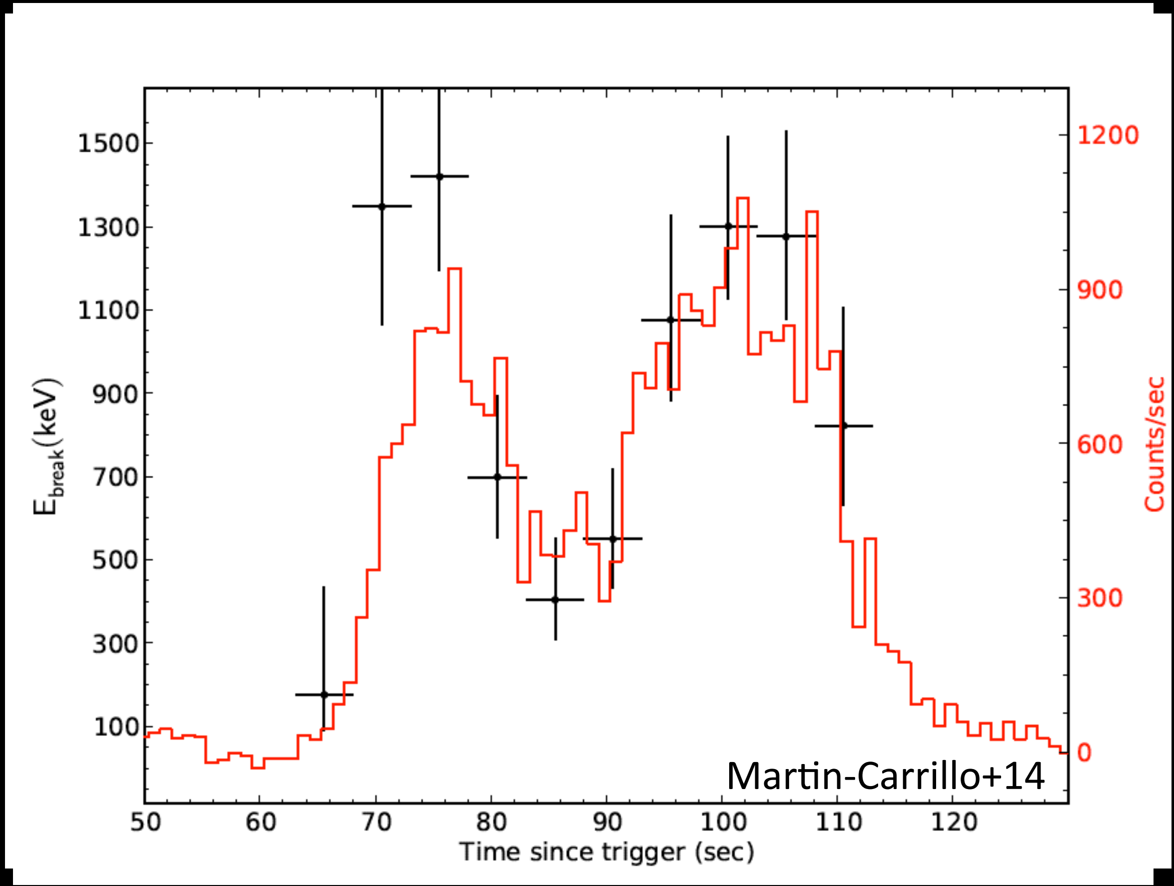

- Very bright event
  - T_{90}~150 s, peak flux=26.7 ph cm^{-2} s^{-1}, fluence 2x10^{-4} erg cm^{-2} (10-1000 keV); Epeak ≈1 MeV!
- Bright optical counterpart peaking at R=12.1 , H=11.9 @ 1-2 minutes after trigger
- Hard X-ray afterglow lasting several ks
- Delayed LAT detection (GeV "afterglow")
- z=1.405

GRB 120711A

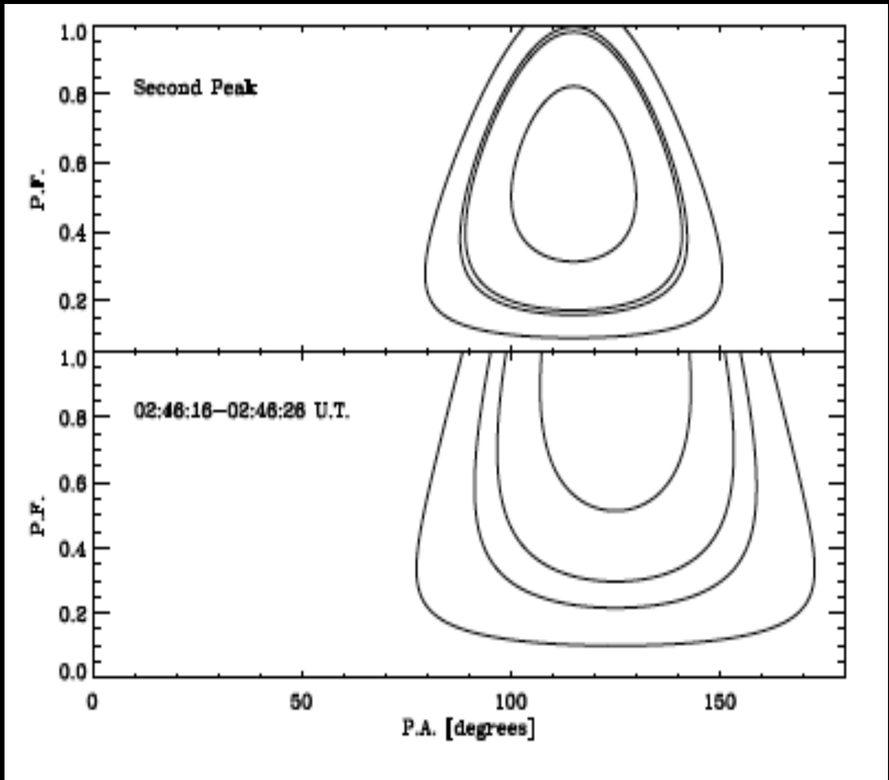

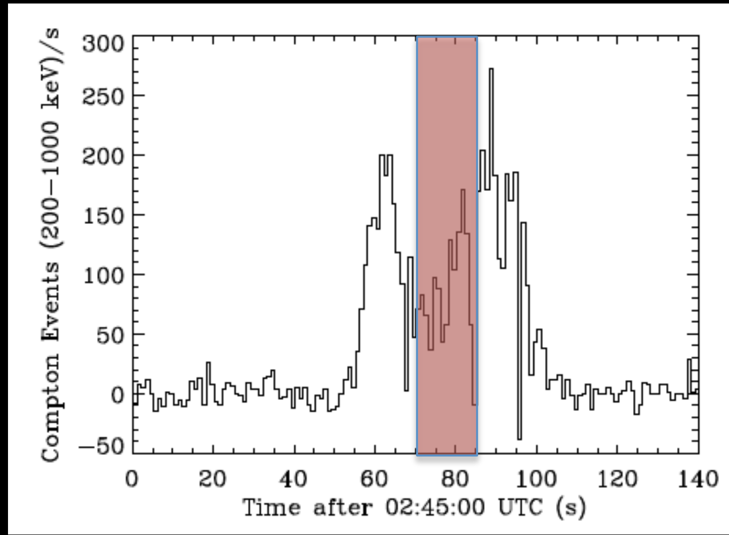

- No polarization signal on the first peak
- Polarization ***only*** on the second peak, and especially its rising part -> interpretation still needed (ICMART?)
- Polarization confirmation by SPI (2 sigma)

Start Time (UTC)	End Time (UTC)	Imaging SNR	PA (°; 68% c.l.)	Π (%; 68% c.l.)	Null-hyp. Prob.
2h46m16s	2h46m26s	10.3	125±20	>37	0.2×10^{-3}
2h46m26s	2h46m36s	14.8	120±20	45±35	1.2×10^{-3}
Second Peak					
2h46m15s	2h46m45s	19.3	115±15	54±27	0.3×10^{-3}

Summary on polarization results

GRB	Π (68% c.l.)	Peak energy (keV)	Fluence and Energy Range (erg cm^{-2})	z	Instrument
041291A	65±26%	201^{+80}_{-41}	2.5×10^{-4} in 20–200 keV	$0.31^{+0.54}_{-0.26}$	IBIS
06122	>60%	188±17	2.0×10^{-5} in 20–200 keV	$1.33^{+0.77}_{-0.76}$	IBIS
100826A	25±15%	606^{+134}_{-109}	3.0×10^{-4} in 20 keV–10 MeV	0.71–6.84[1]	GAP
110301A	70±22%	107±2	3.6×10^{-5} in 10 keV–1 MeV	0.21–1.09[1]	GAP
110721	84^{+16}_{-28}%	393^{+199}_{-104}	3.5×10^{-4} in 10 keV–1 MeV	0.45–3.12[1]	GAP
140206A	>48%	98±17	2.0×10^{-5} in 15–350 keV	2.739±0.001	IBIS

[1] redshift based on empirical prompt emission correlations, not on afterglow observations.

Götz+14

GRB	P.F. (68% c.l.)	Fluence	Peak Energy	Z	Instr.
120711A	54+/-27 %	3.8×10^{-4} erg/cm^2 (20 keV – 10 MeV)	~ 1 MeV	1.405	IBIS

Constraints on LIV

On general grounds one expects that the two fundamental theories of contemporary physics, the theory of General Relativity and the quantum theory in the form of the Standard Model of particle physics, can be unified at the Planck energy scale. This unification requires to quantize gravity, which leads to very fundamental difficulties: one of these is the possibility of *Lorentz invariance violation*

A possible experimental test of LIV is

Testing the helicity dependence of the propagation velocity of photons

Such a test that has already been performed using the SPI measurement of Crab polarization (Maccione+08)

Constraints on LIV

In this some QG theories the light dispersion relation is given by:

$$\omega^2 = k^2 \pm \frac{2\xi k^3}{M_{Pl}} \equiv \omega_\pm^2$$

$$\omega_\pm = |k|\sqrt{1 \pm \frac{2\xi k}{M_{Pl}}} \approx |k|(1 \pm \frac{\xi k}{M_{Pl}})$$

$$\Delta\theta(p) = \frac{\omega_+(k) - \omega_-(k)}{2} d \approx \xi \frac{k^2 d}{2M_{Pl}}$$

M_{Pl}: reduced Planck scale ($2.4\ 10^{18}$ GeV)

For the Crab:
$\xi < 2\ 10^{-9}$

GRB : at least 10^5 times further away

Constraints on LIV

- GRB 041219A: z = 0.31 $^{+0.54}_{-0.26}$; d = [0.222-5.406] Gpc (photometric)

$\xi < 1.1 \times 10^{-14}$ *Laurent+11*

- GRB 061122: z = 0.57<z<2.10; d>3.3 Gpc (photometric)

$\xi < 3.4 \times 10^{-16}$ *Götz+13*

- GRB 140206A: 2.739+/-0.001; d=23 Gpc (spectroscopic!)

$\xi < 1.0 \times 10^{-16}$ *Götz+14*

Crab Nebula

Forot+11, Moran+13

Crab Light Curve

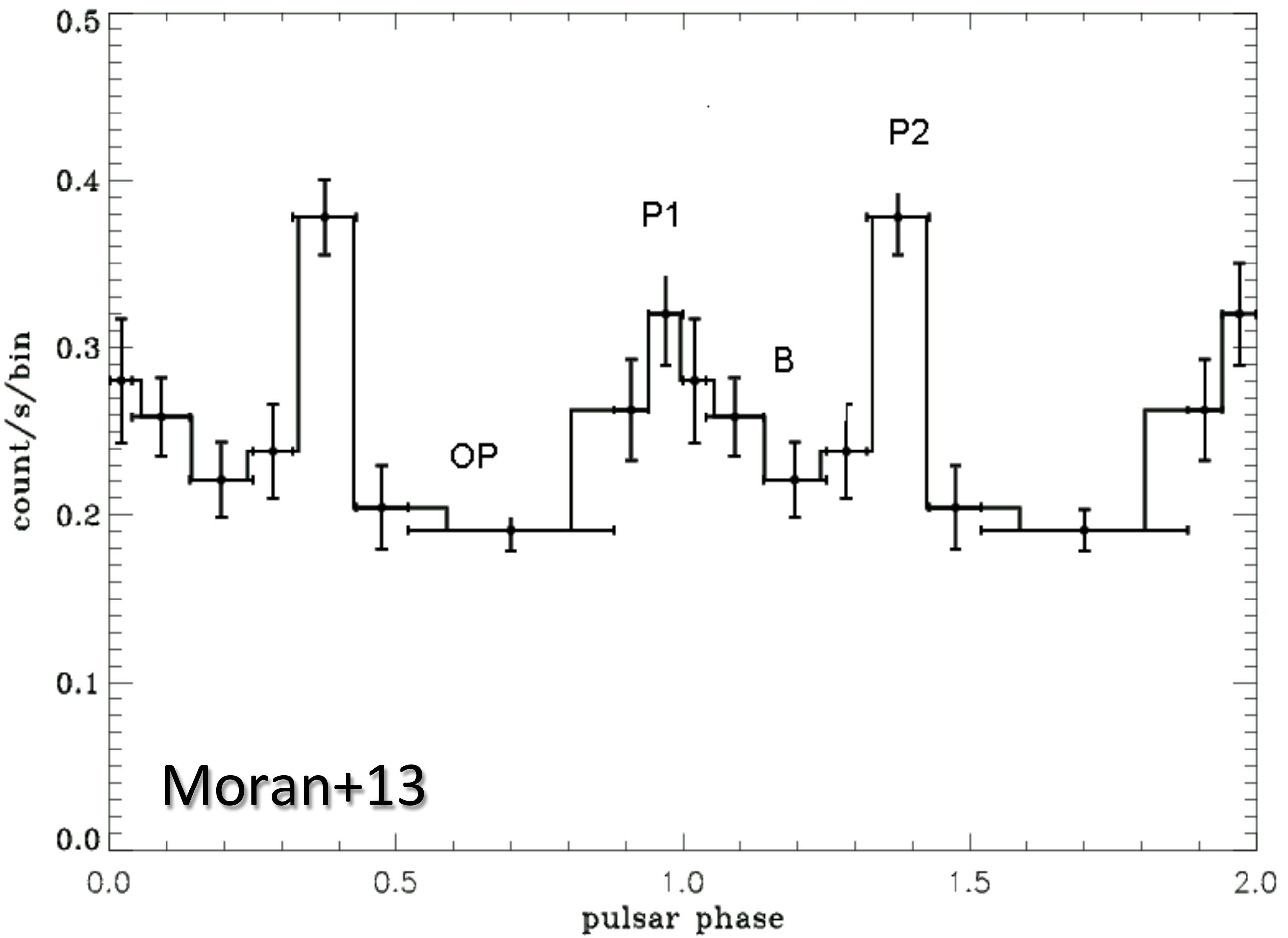

P_1	$0.88 < \Phi < 0.14$
B	$0.14 < \Phi < 0.25$
P_2	$0.25 < \Phi < 0.52$
OP	$0.52 < \Phi < 0.88$

Phases according to Kuiper+01

IBIS Crab Reuslts

- Phase Averaged Results

	Moran+13	Forot+08	Chauvin+13
Observation time	2.6 Ms	1.2 Ms	0.6 Ms
Polarisation Position Angle (°)	85 ± 10	100 ± 11	117 ± 9
Polarisation Fraction	0.58 ± 0.07	$0.47^{+0.19}_{-0.13}$	28 ± 6

- **Phase Resolved Results (Forot+08)**

Phase	Pol. Fraction	Pol. Angle (°)	Prob.
P1+P2	$0.42^{+0.30}_{-0.16}$	70 ± 20	3.3×10^{-2}
Off Pulse	> 0.72	120 ± 9	2.6×10^{-4}
Off Pulse+Bridge	> 0.88	122 ± 8	1.0×10^{-4}

Optical Results

HST ACS

M

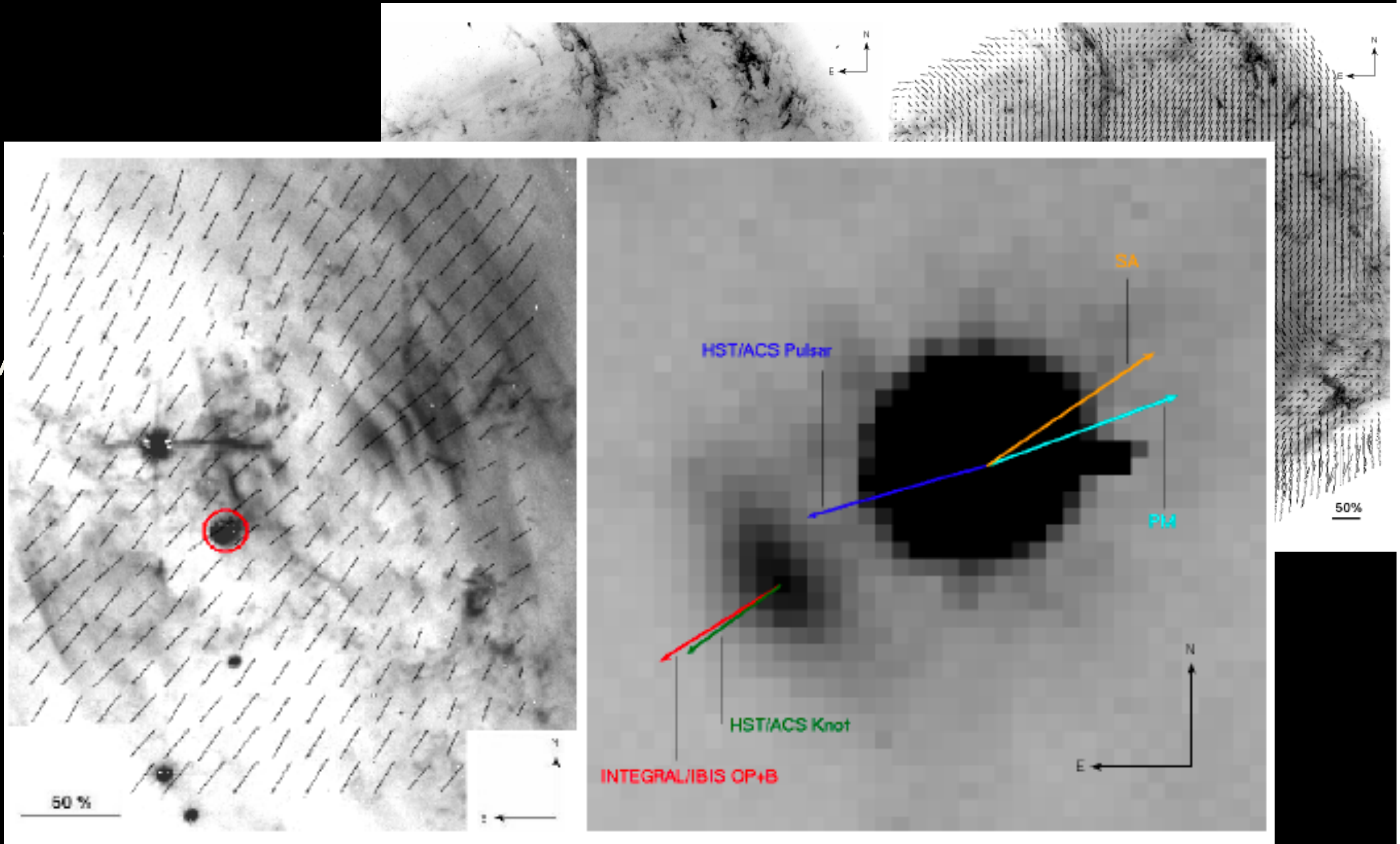

Multi wavelength Results

	Polarisation (%)	Position Angle (°)
[1] γ-ray SPI OP	46 ± 10	123 ± 11
[2] γ-ray IBIS OP	> 72	120.6 ± 8.5
[2] γ-ray IBIS OP+B	> 88	122.0 ± 7.7
[2] γ-ray IBIS $P_1 + P_2$	$42 \pm^{30}_{16}$	70 ± 20
[3] Optical (OPTIMA) *pulsar*	9.8 ± 0.1 (~5% -DC)	109.5 ± 0.2 (96.4 -DC)
[4] Optical (HST) *pulsar*	4.90 ± 0.33	105.97 ± 2.00
[4] Optical (HST) *knot*	61.70 ± 0.72	126.86 ± 0.23
[5] X-ray (2.6-5.2 Kev) *nebula*	19.22 ± 0.92	155.79 ± 1.37

[1] Dean+08
[2] Forot+08
[3] Słowikowska+09
[4] Moran+13
[5] Weisskopf+77

The knot may be responsible for the gamma ray polarized emission. Time resolved optical measurements obtained by GASP may settle the question, Moran et al. in prep

Cyg X-1

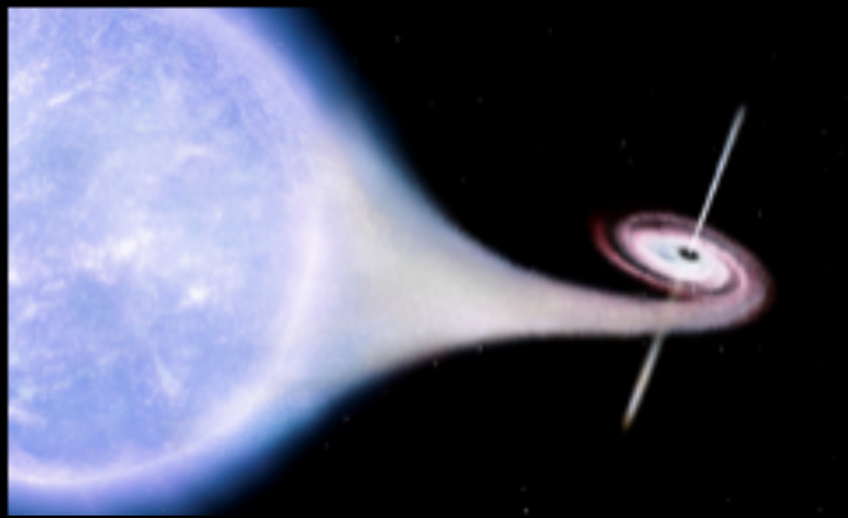

Laurent+11, J. Rodriguez+ subm.

Cyg X-1 Results

- All Cygnus X-1 data from 2003 to 2009 for a total of 5 Ms.
- All IBIS data over all Cygnus X-1 spectral states. A more detailed analysis making selection according to the source states is on-going (Rodriguez et al. in preparation).
- Analysis made in 6 bins in φ azimuth (0° ≤ ϕ ≤ π).

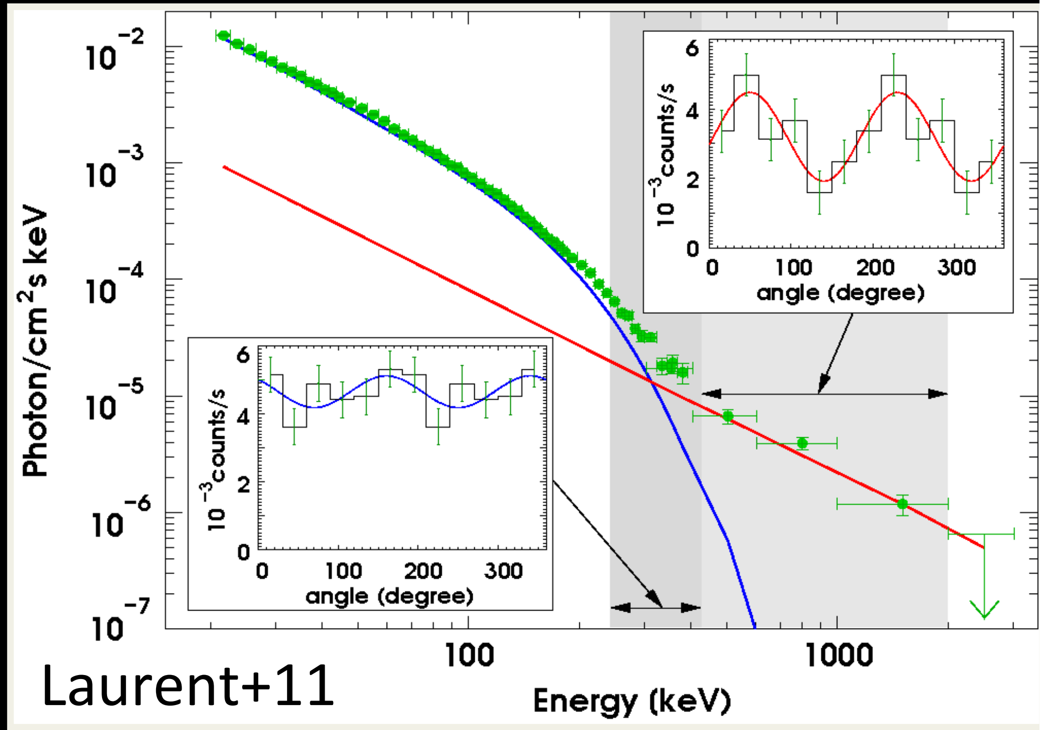

Polarization fraction : 67 ± 30 % (90 % c.l.)

Polarization angle: ~~140 ± 15°~~ → 40 ± 15°

SPI P.F. = 76 ± 15 % P.A. = 42 ± 3° (Jourdain+12)

Cyg X-1: time resolved analysis (Rodriguez et al. subm.)

Radio and Hard-X ray long term monitoring of the source

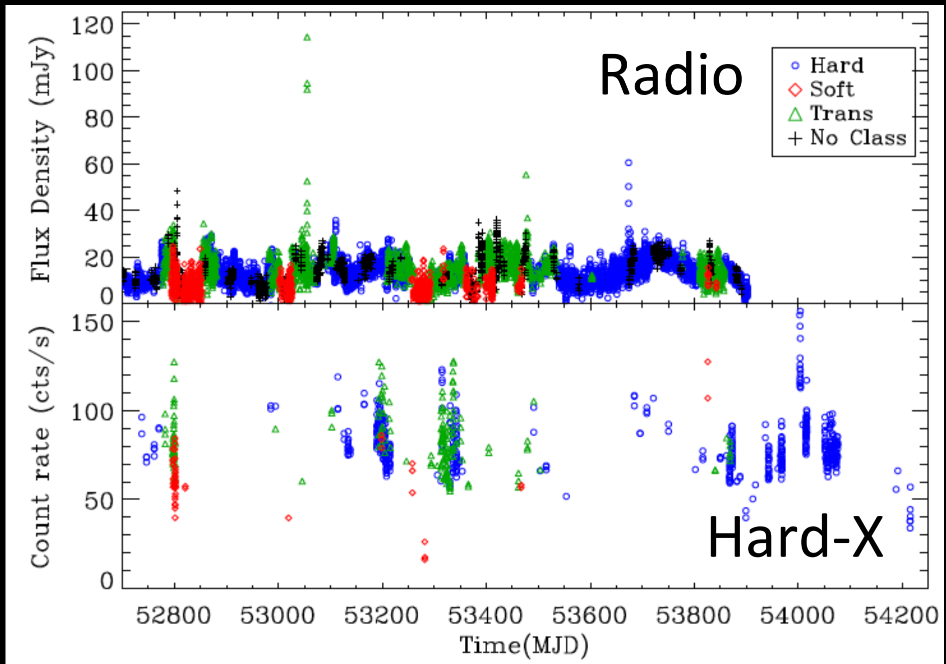

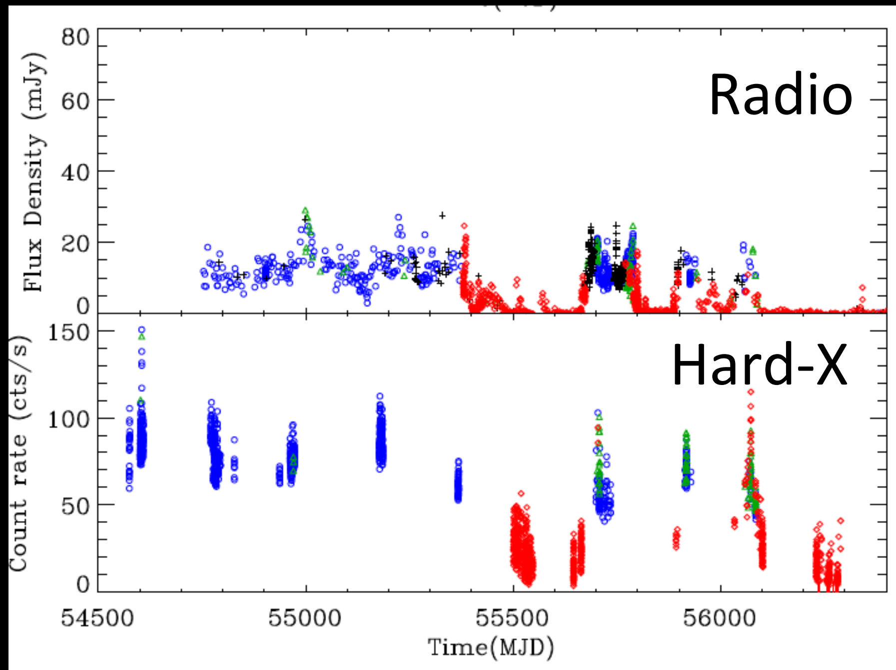

Cyg X-1: time resolved analysis

INTEGRAL spectra

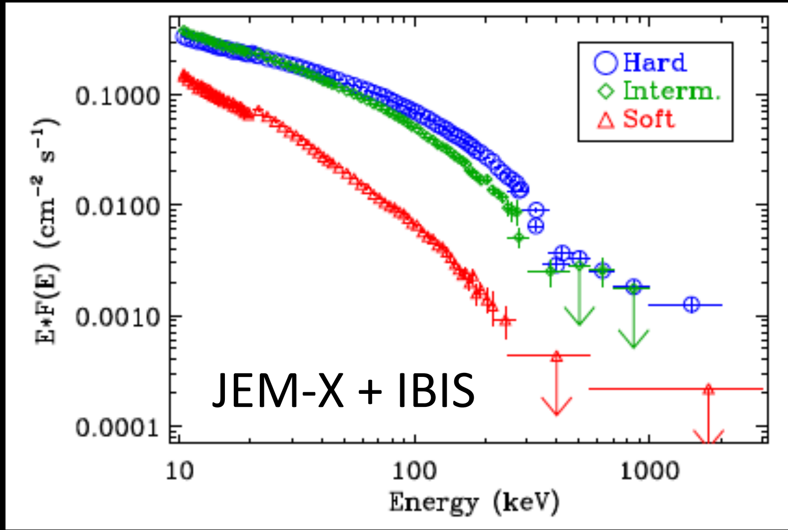

TABLE 1

SPECTRAL PARAMETERS OF FIT TO THE 10–400 KEV SPECTRA. ERRORS AND LIMITS ON THE SPECTRAL PARAMETERS ARE GIVEN AT THE 90% CONFIDENCE LEVEL, WHILE THE ERRORS ON THE FLUXES ARE AT THE 68% LEVEL.

reflect*highecut(powerlaw)						
State	Γ	E_{cut} (keV)	E_{fold} (keV)	Fluxes‡ 10–20 keV	20–200 keV	200–400 keV
LHS	1.43 ± 0.01	≤ 12	155 ± 4	4.48 ± 0.02	22.30 ± 0.03	3.56 ± 0.03
IS	$1.87^{+0.02}_{-0.03}$	56^{+4}_{-6}	198 ± 8	5.10 ± 0.03	18.47 ± 0.04	2.52 ± 0.05
HSS†	2.447 ± 0.007	130^{+11}_{-16}	198^{+135}_{-59}			
reflect*comptt						
State	$\Omega/2\pi$	kT_e (keV)	τ	Fluxes‡ 10–20 keV	20–200 keV	200–400 keV
LHS	0.13 ± 0.02	$59.4^{+1.3}_{-1.2}$	1.06 ± 0.03	4.37 ± 0.03	22.60 ± 0.03	3.70 ± 0.03
IS	0.04 ± 0.03	$54.4^{+3.6}_{-2.8}$	0.82 ± 0.06	5.30 ± 0.03	18.42 ± 0.06	1.93 ± 0.07
HSS	0.36 ± 0.03	279 ± 15	< 0.013	1.84 ± 0.09	3.7 ± 0.6	0.4 ± 0.1

† A reflection component with $\Omega/2\pi$=0.46±0.04 was included for a good spectral fit to be obtained

‡ In units of 10^{-9} erg cm^{-2} s^{-1}

Cyg X-1: time resolved analysis

Polarization Results: a detection is obtained only in LHS; unconstraining U.L. in IS and HSS (~6 sigma detection in the Compton mode)

P.F.$_{LHS}$= 82±38% P.A.$_{LHS}$= 40±5° => the 2011 result was dominated by LHS.

FIG. 4.— Polarigrams obtained in the LHS. Note the different vertical scales. In both panels the horizontal line shows a zero level of polarization fraction. **Left:** 300–450 keV. **Right:** 450–2000 keV.

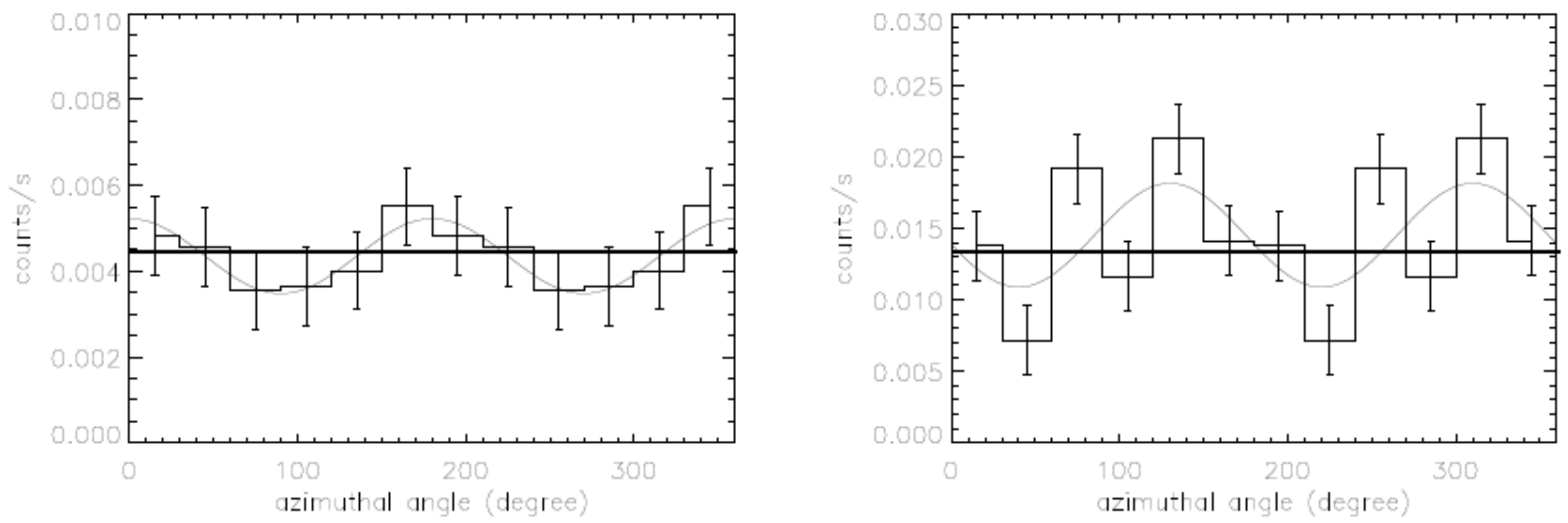

Cyg X-1: time resolved analysis

Polarization Results: a detection is obtained only in LHS; unconstraining U.L. in IS and HSS (~6 sigma detection in the Compton mode)

$P.F._{LHS}$= 82±38% $P.A._{LHS}$= 40±5° => the 2011 result was dominated by LHS.

The high degree of polarization of the hard tail most probably originates from synchrotron emission in an highly ordered magnetic field.

The demonstrated presence of radio emission (likely due to a compact jet) in the LHS points towards the compact jet as the origin for the 0.4-2 MeV emission corroborating theoretical and multi-wavelengths studies presented by other teams (Malyshev+13; Russell & Shahbaz 2013).

Conclusions

- INTEGRAL has shown the potential of polarization studies for persistent sources and GRBs (including fundamental physics!), introducing a new parameter space (after timing and spectroscopy) through which bright HE sources can be studied

- Multi wavelength observation campaigns on the Crab nebula have confirmed the IBIS results, helping to identify the origin of the polarized emission

- Time resolved studies on Cyg X-1 are starting to shed light on the astrophysical processes in the LHS.

- Concerning GRBs: IBIS has detected polarized signals from 4 GRBs. Like IBIS (and SPI), the Japanese GAP experiment on the solar wind sailing platform IKAROS has confirmed the detection of polarization in three bright GRBs (see D. Yonetoku's presentation). Although individually not extremely significant (3-4 sigma) IBIS, SPI and GAP ***independent*** results point toward a high level of polarization in the prompt emission of GRBs.

- Next generation polarimeters (e.g. POLAR, POET, GEMS, XIPE, HARPO, etc.) will be of paramount importance to better constrain the physical mechanisms at work in HE sources.

- X/gamma-ray polarization: a window about to open? **YES!**